Nature of the Flow-Induced Worm Texture of Thermotropic Polymers

T. De'Nève,† P. Navard,*,‡ and M. Kleman§

DGA/CREA, 16 bis Avenue Prieur de la Côte d'Or, F-94114 Arcueil Cedex, France, Ecole des Mines de Paris, URA CNRS No. 1374, Centre de Mise en Forme des Matériaux, BP 207, F-06904 Sophia–Antipolis Cedex, France, Laboratoire de Physique des Solides, Université de Paris-Sud, Bât. 510, F-91405 Orsay Cedex, France, and Laboratoire de Minéralogie–Cristallographie, Université Pierre et Marie Curie, Tour 16, Case 115, 4 Place Jussieu, F-75252 Paris Cedex 05, France

Received February 18, 1994; Revised Manuscript Received October 7, 1994⊗

ABSTRACT: Nematic polymers show at low shear rates the so-called worm texture which is characterized by a large density of defects. To study these defects, a specially designed cone-and-plate rheometer has been used for quenching the flowing worm texture of a thermotropic polymer. The preparation of samples involves ultramicrotoming and etching with sulfuric acid. The observations show that the defects are half-integer twist disclination loops lying in the shearing plane. The director is oriented along the flow direction inside the loop and along the vorticity axis outside.

Introduction

The texture displayed at rest by nematic polymers is the thread texture. It contains very few defects. Their strength and character can be determined by optical microscopy. Once a weak shear flow is applied on such a texture, there is a sudden and strong increase in the defect density. The texture thus developed is the so-called worm texture.[1] Very little is known about the defects which are present in this texture because a direct optical study is hampered by the difficulty of isolating such moving objects.[1,2]

This texture is a characteristic response of polymers, either lyotropic or thermotropic, to a weak shear flow. It is related to the flow mechanism of nematic polymers. The molecular rheological theory of Doi[3] was created for lyotropic rodlike polymers in the isotropic and anisotropic states. It was then modified by Marrucci and Maffetone.[4] Their two-dimensional numerical simulation in the shearing plane has first shown that a periodic rotation of the director, the so-called tumbling, occurs at low shear rates. The three-dimensional numerical approach of Öttinger and Larson[5] has shown that, at low shear rates, the director reaches two attractors. The first one is the shearing plane and the second one is the vorticity axis. Tumbling is also shown to occur in three dimensions, but in a more complex manner, carrying both in-plane and out-of-plane components. These theories can predict most of the rheological properties of nematic polymers such as the occurrence of negative values of the first normal stress difference at intermediate shear rates. However, these theories do not take defects into account. They play a major role, since their presence completely modifies the nature of the dissipative phenomena which occur during shear. They can also result from fundamental modes of instability of the homogeneous distortions, as described by Marrucci and Greco.[6] It is well known that the rheological behavior of solids arises from defects and that the different stages of deformation reveal universal features which depend in a unique way on the structure (bcc, fcc, etc.).[7] Similarly, the different stages of deformation of ordered liquids, here nematic polymers, should have some degree of universality.

In order to study the defects of the worm texture, a well-characterized thermotropic polymer, Vectra B950, has been chosen. Its texture at rest has been recently characterized[8] as well as its rheological behavior.[9] In addition, the relationships between the various textures found during flow and the rheological behavior have been described.[9] In particular, the conditions for which a wormlike texture appears have been determined in terms of shear rate and shear strain. A preliminary report[10] shows that the defects are mostly half-integer twist disclination loops. The defect density has also been measured as a function of shear rate and shear strain.[11,12]

The purpose of this paper is to describe the nature of the defects found in the wormlike texture of this thermotropic polymer. In particular, their position in the flow gradient, the director arrangement around the core, and the nature of the core will be addressed. The relationship of these defects with the rheology will be discussed and compared with rheological theories.

Experimental Section

Material. The material used is a thermotropic copoly(ester amide) based on 60/20/20 6-hydroxy-2-naphthoic acid/hydroxybenzoic acid/aminophenol. It is supplied by Hoescht-Celanese under the trade name Vectra B950. The melting temperature is about 290 °C and its molecular weight is about 20 000.

Cone-and-Plate Apparatus. A cone-and-plate apparatus, previously designed by F. Lequeux in Orsay, was adapted to quench the flowing worm texture of the thermotropic polymer. The plate diameter is 51 mm and the cone angle 3°. The parallelism between the cone and the plate and the accuracy of the gap were carefully checked. This apparatus is equipped with a heating chamber consisting of two semicylindrical parts that can quickly part. Before flow, a cut squared sample obtained from an injection-molded plate was placed between the cone and the plate at 300 °C and consecutively compressed. A rest time of 15 min was allowed before the test took place. The shear rate used was 1 s^{-1}, which is in the shear rate range where only the worm texture exists.[9] The total shear strain applied to the material is also an important factor since the worm texture appears only above a critical shear strain.[9] The number of revolutions of the cone that was imposed to a sample

* To whom correspondence should be sent.
† DGA/CREA.
‡ Ecole des Mines de Paris.
§ Université de Paris-Sud and Université Pierre et Marie Curie.
⊗ Abstract published in *Advance ACS Abstracts,* January 1, 1995.

0024-9297/95/2228-1541$09.00/0

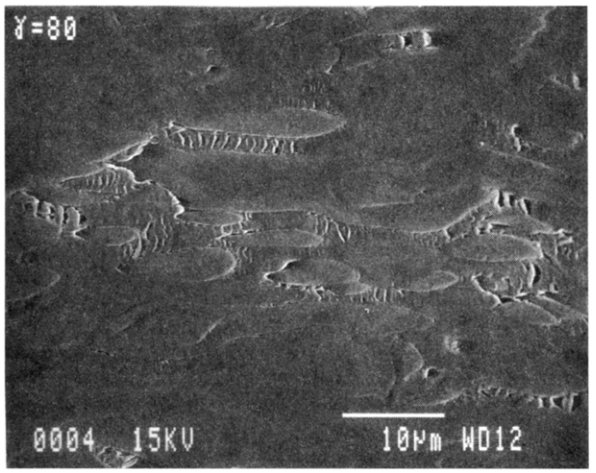

Figure 1. Scanning electron micrograph of the surface ultramicrotomed parallel to the shearing plane. The cutting direction is parallel to the flow direction. The sample was sheared during 80 shear strain units at 1 s^{-1}. The flow direction is horizontal, and the gradient direction is vertical.

was precisely controlled. When a given number of revolutions, corresponding to the shear strain chosen, was completed, the cone rotation was automatically stopped by a diode-control system. The heating chamber was then automatically and quickly opened, and a flow of water was immediately pushed in the cone and the plate area to quench the sample. The sample was then removed at room temperature from the gap between the cone and the plate.

Observations of the Polymer. At 1 s^{-1}, the worm texture appears above 12 shear strain units.[8] The applied shear strain before quenching was therefore chosen above this critical value. The cone-shaped samples obtained after removal from the cone-and-plate apparatus were cut with a Reichert-Jung ultramicrotome equipped with a diamond knife. Three perpendicular cut planes were chosen. The first one is the plane perpendicular to the flow direction, containing the vorticity axis and the shear gradient. The second one is the shearing plane, containing the shear gradient and the flow direction. The third one is perpendicular to the other two, containing the flow direction and the vorticity axis. Two types of samples were obtained. The first type was the cut, with a thickness of 0.2 μm. It was observed by optical microscopy with a Leitz microscope. The second type was the bulk sample, whose surface was ultramicrotomed and was thus very smooth. This cut surface was observed by scanning electron microscopy with a JEOL microscope either "as cut" or after etching with sulfuric acid. The ultramicrotomed bulk samples were etched during different durations of time. The most suitable duration time depends on the cut plane. It was a few minutes for the plane perpendicular to the flow direction and a few tens of seconds for the other two. Longer durations of time were found to damage the surface. It was reported in the literature that etching may produce ridges either parallel or perpendicular to the chains[13,14] and that such a method has been applied to investigate defect morphology during shear flow.[15,16]

Results

Scanning Electron Microscopic Observations. Virgin Surface. The surface cut perpendicular to the flow of a sample sheared during either 14 or 80 shear strain units does not display any clear structure. It looks violently perturbed by the cutting process.

The surface cut parallel to the shearing plane is very different. It displays loops elongated in the flow direction (Figure 1). The features of these loops do not change along their contour, suggesting that they lie inside the shearing plane. They are surrounded most of the time by fractures on their external part. An analysis of the profile of these cracks (see Figure 2) is given elsewhere.[10] It was shown that the cracks are mostly parallel to the cut surface.

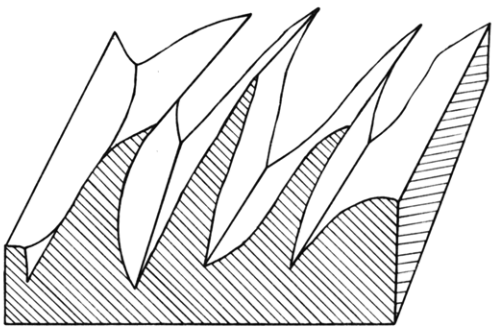

Figure 2. Profile of the cracks obtained by stereomicroscopy. The flow direction is horizontal, the vorticity axis is vertical, and the gradient direction is perpendicular to the plane of the figure.

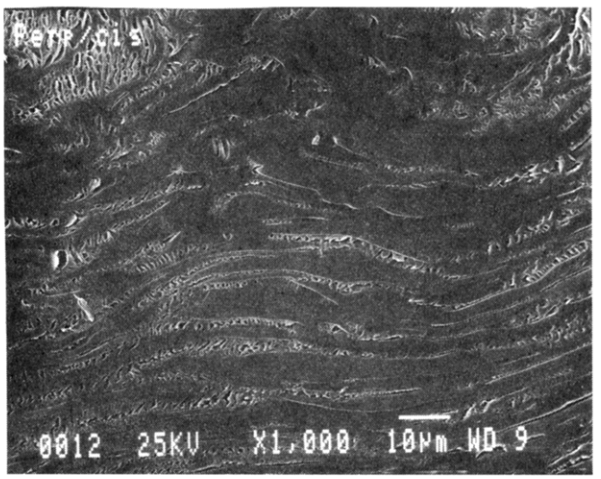

Figure 3. Scanning electron micrograph of the ultramicrotomed surface cut parallel to the flow direction and vorticity axis. The sample was sheared during 80 shear strain units at 1 s^{-1}. The cutting direction is parallel to the flow direction. The flow direction is horizontal, and the vorticity axis is vertical.

The surface cut along the plane containing the flow direction and the vorticity axis shows the existence of lines elongated along the flow direction (Figure 3). They are therefore the images of the loops contained in the shearing plane. At some places, half-integer wedge disclination lines transversal to the cut can be observed (Figure 4).

Surface of Samples Etched with Sulfuric Acid. The surface cut parallel to the shearing plane reveals the existence of various cylindrical "objects" which pop up from the bulk after etching. At first sight, they belong to three classes of "objects":

The objects of the first class are the loops previously observed (Figures 5–8). The "end" of the loops in the flow direction is like a nipping of the rods.

A very important difference is observed between the loops corresponding to $\gamma = 14$ and $\gamma = 80$. At $\gamma = 14$, a rolled pattern is observed (Figure 8), with opposite rolling sense on opposite sides of the same loop. This rolled pattern is most certainly due to the chains which are also in this configuration. At $\gamma = 80$ (Figures 5 and 6), this rolled pattern is generally not observed, except for the objects of the second and third classes described below. These loops have a fibrillar character, suggesting that the chains are aligned parallel to these loops when they are close to them.

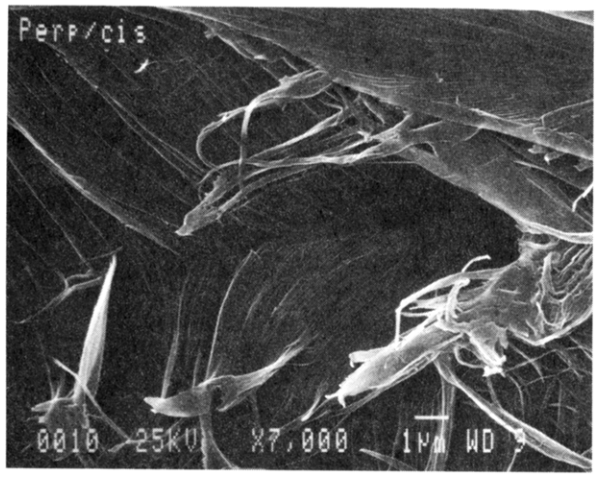

Figure 4. Magnification of Figure 3. The cutting direction is parallel to the flow direction. The flow direction is horizontal, and the vorticity axis is vertical.

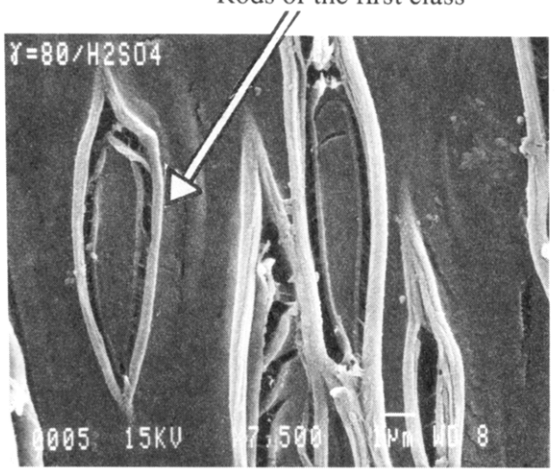

Figure 5. Scanning electron micrograph of the surface cut parallel to the shearing plane and etched with sulfuric acid during 20 s. The sample was sheared during 80 shear strain units at 1 s^{-1}. The cutting direction is parallel to the flow direction. The gradient direction is horizontal, and the flow direction is vertical.

A few loops terminate in the flow direction with rods which are perpendicular to the flow (Figure 6). These few loops do not show the same fracture pattern as the ones described before. When there is a nipping, there is a separation between the etched surface and the rods *inside* the loop for *all parts of the loop*. When no nipping is observed, this separation is *outside* the loop *for one segment of the loop*. We have no clear explanation for such a difference but it is likely that these loops are of a different nature from the ones discussed in this paper.

The objects of the second class are lips (Figure 6) which are observed at $\gamma = 14$ and $\gamma = 80$. These lips are made by two fibrillar parts around which the chains are rolled in opposite directions. The two parts of the lips are very close to each other.

The objects of the third class (Figures 9 and 10) bear some similarities to those of the first two classes. They originate from the addition of two parts of a loop of the first class at a point where they are covered up by a rolled pattern (Figure 9). However, an important difference between the rolled pattern of these objects and the ones of the second class is that the direction of rolling is now the same on the two parts. A magnification (Figure 10) of these objects when they are still

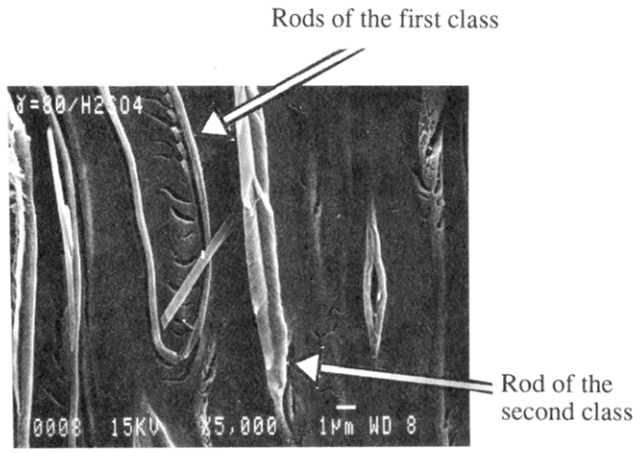

Figure 6. Scanning electron micrograph of the surface cut parallel to the shearing plane and etched with sulfuric acid during 20 s. The sample was sheared during 80 shear strain units at 1 s^{-1}. The cutting direction is parallel to the flow direction. The gradient direction is horizontal, and the flow direction is vertical.

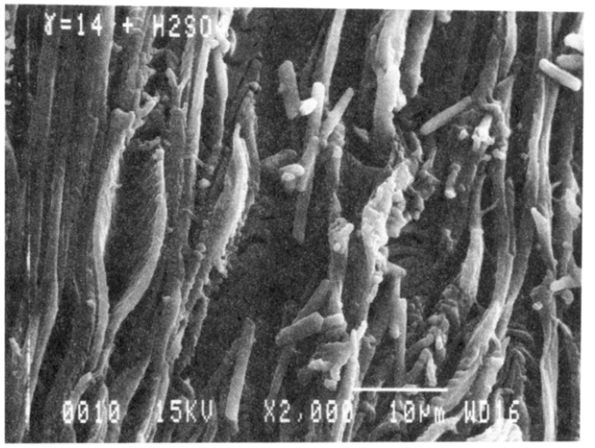

Figure 7. Scanning electron micrograph of the surface cut parallel to the shearing plane and etched by sulfuric acid during 40 s. The sample was sheared during 14 shear strain units at 1 s^{-1}. The cutting direction is parallel to the flow direction. The gradient direction is horizontal, and the flow direction is vertical.

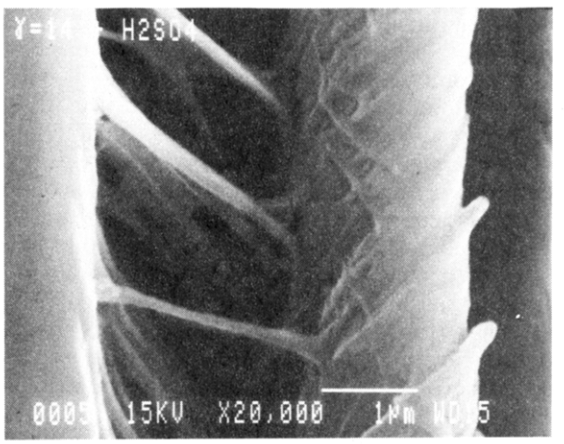

Figure 8. Magnification of Figure 7. The gradient direction is horizontal, and the flow direction is vertical.

attached to the surface shows that they separate two areas which bear exactly the same fracture profile. Close to this object, a fibrillar pattern is observed, showing that the neighboring chains are aligned parallel to the object. The size of these defects seems to depend on the shear strain γ. At $\gamma = 80$ the defects are 2−3

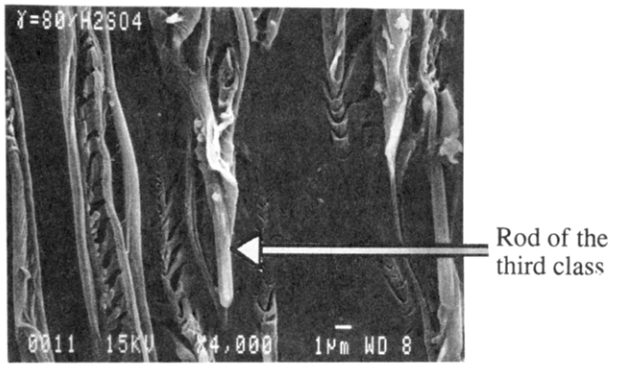

Figure 9. Scanning electron micrgraph of the surface cut parallel to the shearing plane and etched with sulfuric acid during 20 s. The sample was sheared during 80 shear strain units at 1 s^{-1}. The cutting direction is parallel to the flow direction. The gradient direction is horizontal, and the flow direction is vertical.

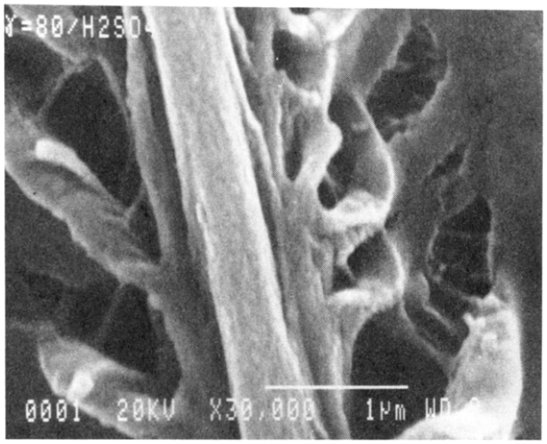

Figure 10. Magnification of Figure 9. The gradient direction is horizontal, and the flow direction is vertical.

times smaller than at $\gamma = 14$ (see the scale on the figures).

Optical Microscopic Observations. The ultramicrotomed cuts were observed by optical microscopy. Those obtained from a cut parallel to the shearing plane show the existence of defect loops, more or less elongated in the flow direction (Figure 11). The external part of the loop remains dark during a complete rotation of the sample between crossed polars. This is compatible with a homeotropic orientation of the chains, i.e., chains oriented along the vorticity axis. In the diagonal position, a gypsum plate was inserted. The change of color from magenta red to blue (in the Newton scale) results from a parallel orientation between the optic axis and the fast component of the wedge. This increase is observed inside the loop. This is compatible with an orientation of the chains along the flow direction. Most interesting is the fact that this increase of color is very large close to the segments of the loops. This shows that the chains are highly oriented along the flow direction, near the core of the defects. This is compatible with the fibrillar pattern of the loops revealed by etching in sulfuric acid.

Discussion

Topological Model of the Defects. One of the major results coming from these observations is the existence of elongated loops which clearly show up on the SEM pictures of virgin surfaces parallel to the shearing plane. These loops are the images of disclination loops. Their density is indeed comparable to that of the defects

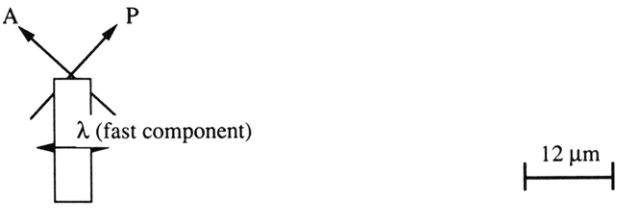

Figure 11. Optical micrograph of an ultramicrotomed cut corresponding to the sample of Figure 1 observed with crossed polars and gypsum plate. The flow direction is along A, and the gradient direction is along P.

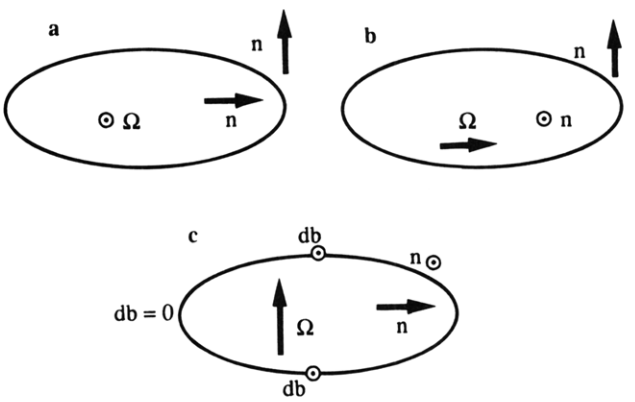

Figure 12. Three possible cases for the character of the disclination loop, depending on the orientation of the rotation vector Ω. The Burgers vector $d\vec{b}$ is oriented as given by eq 1. For each case, the orientation of the director $\vec{n}$ inside and outside the loop can be interchanged. The flow direction is horizontal, and the gradient direction is vertical.

of the worm texture. The aspect of these loops being the same along their contour, they lie inside the shearing plane. This is also supported by scanning electron microscopy observations of the plane containing the flow direction and the vorticity axis, which show the existence of lines elongated in the flow direction (Figure 3).

The difference between the inside and outside parts of the loops suggests that they are half-integer disclinations. If it is so, three main configurations are possible: either the rotation vector $\vec{\Omega}$ which builds the defect is perpendicular to the shearing plane (the loop is then a twist loop (Figure 12a)) or $\vec{\Omega}$ is in the shearing plane (the loop segments along the flow direction are then either of a wedge (Figure 12b) or of a twist character (Figure 12c). For each case on Figure 12, the orientation of the director $\vec{n}$ inside and outside the loop can be interchanged. The first and second types imply that most of the directors are aligned in the gradient direction, a fact not likely to occur in a shear flow and not supported by optical observations (Figure 11).

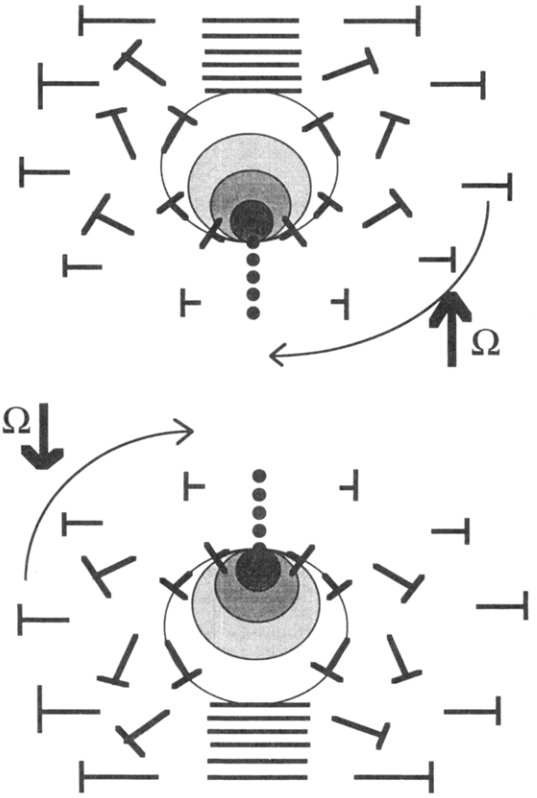

Figure 13. Model of the core of the defects. $\vec{\Omega}$ is the rotation vector of the director when moving on a closed circuit around the defect.

The third hypothesis is therefore likely to be the correct one. It also has the advantage of explaining the profile of the fractures (Figure 1). The transversal profile of the cracks (Figure 2) was determined by stereomicroscopy.[10] It shows that the plane of these cracks is mostly parallel to the cut surface. In addition, the orientation of the plane of the cracks is the same on both sides of the loop. These peculiar features can be explained as follows. The distortions of the director field carried by a twist disclination segment dl imply the presence of a dislocation density $d\vec{b}$. If the dislocations do not carry stresses in the nematic state, this is no longer true in a frozen nematic, in which they act as sources of stress. The Burgers vector density $d\vec{b}$ along a line element of length dl is defined by[17]

$$d\vec{b} = \vec{L} \wedge \vec{\Omega}\, dl \qquad (1)$$

where $\vec{L}$ is the disclination line unit vector. In the present case, eq 1 implies that the Burgers vectors are perpendicular to the surface of observation. Assuming that the stress relaxation due to dislocations leads to a cleavage in such a polymeric system, the plane of the cracks would be parallel to the surface, yielding a sort of "fish scale" pattern. This is exactly what is observed.[10] Equation 1 also defines the sign of the Burgers vector, as shown in Figure 13: it is the same on both sides of the loop. This explains why the two profiles along parallel lines taken on both sides of the same loop have the same shape. A possible explanation is that the observed objects are half-integer disclination loops contained inside the shearing plane. These loops separate chains oriented along the vorticity axis *outside* the plane of the loop from chains oriented parallel to the flow *inside* the loop, in agreement with what is seen in the optical observations of the cuts (Figure 11). The rotation vector $\vec{\Omega}$ being oriented in the gradient direction, such loops have mostly a twist character, except for the segments of the loop perpendicular to the flow, where they have a wedge character. This is why half-integer wedge lines are sometimes observed on the surface cut parallel both to the flow direction and the vorticity direction (Figure 4). However, this wedge character seems to be unfavored since a nipping generally terminates the loops in the flow direction. We shall comment further on other kinds of defect lines present in our specimens.

Structure of the Core. The loops revealed by etching in sulfuric acid can help to give an indication of the director arrangement close to the core of the disclination line. These rods follow the contour of the disclination loops. They are most probably the cores of the defects. Etching reveals the loops by attacking the surrounding material, which most certainly points to the fact that the molecular packing is much better in the core. The core has a fibrillar aspect. By analogy with the etching of semicrystalline polymers, this means that the chains are highly oriented near the core. The same conclusion is also drawn when looking at the optical micrographs of the ultramicrotomed cuts. All these facts indicate that the core is composed of a perfect nematic (probably a biaxial nematic), a hypothesis previously made by Mazelet *et al.*[18] for another thermotropic polymer. See also a recent Monte Carlo simulation of the core of a disclination in a solution of nematic rods which points toward a similar effect.[19] The rolled disposition of the chains around the core allows us to propose the model shown in Figure 13. The direction of the rolling around the core defines the sign of the disclination.

A remarkable feature of these cores is their large macroscopic size, of the order of a micron. This is probably related to the fact that the lines are in motion. They may move by dragging a large amount of nematic fluid in order to minimize distortion energy. A similar observation has also been reported for disclinations in small-molecule nematics.[20]

Object of the Third Class. Coming now to the objects of the third class, they most probably are the cores of integer disclination lines, since they originate from the addition of two half-integer disclination lines (Figure 9). This is supported by the fact that on Figure 9, the left and right areas separated by such a defect have the same fracture profile after etching. The fact that they do not close is also coherent with their integer character. The termination of this type of loop is a singular point which marks the transition between a singular integer disclination and a nonsingular evanescent one (escape in the third direction).[21]

Relationship with the Rheological Regime. The most interesting result of this work is the finding that defects are created by shearing a nematic polymer. Starting with a nearly defect-free sample, a huge quantity of defects appears after some shear strain.[9,11,12] Shear, at least at low shear rates, disorders the nematic fluid. This can be related to a nonaligning behavior of the director, as in the theoretical model of tumbling nematic polymers.[4-6] In this model, the director undergoes a continuous motion in the shearing plane if the director has been initially positioned in this plane or a complex motion if the director has a component out of the shearing plane. Such motions are probably unstable in some way and could yield a production of defects. According to ref 22, an equilibrium density of defects should thus be obtained when the distance

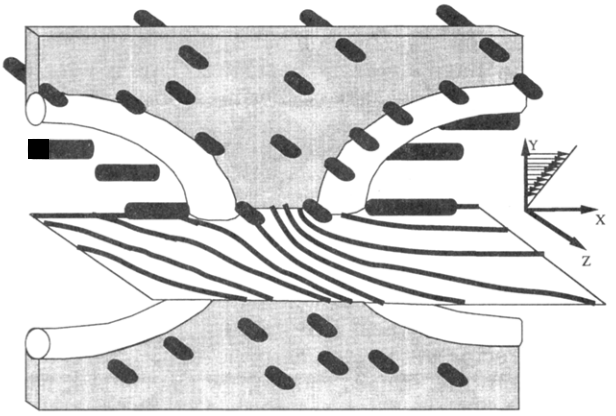

Figure 14. Model of the worm texture. The small black rods represent the chains. The thick gray rods represent the core of the disclination. X is the flow direction, Y is the gradient direction, and Z is the vorticity axis.

between neighboring defects stops the tumbling tendency. For another point of view, see also Larson and Mead.[23] This equilibrium density is reached after a long time through the creation and annihilation of defects.[9]

The defects which have been found are mostly loops. If such a mechanism is universal for tumbling nematic polymers, it should also occur for lyotropics. These defects should therefore be the scattering objects that give the peculiar four-leaf and streak depolarized scattering pattern found for lyotropics and some thermotropics.[2,25,26] Preliminary works along this line show that the theoretical prediction of the scattering by these loops is compatible with the observed patterns.[27]

The orientation of the director around the defect loops is schematized in Figure 14, as it can be inferred from our results. The director is along the flow direction inside the loop and along the vorticity direction outside. This yields the hypothesis that, at low shear rates, the director is mostly oriented along the vorticity axis and that the further appearance of disclination loops as the shear rate increases imposes an ever increasing orientation in the flow direction. This is compatible with orientation measurements by X-ray scattering during flow on lyotropics and thermotropics.[28–30] At high shear rates, the volume of vorticity becomes small and confined outside the plane of the loops, between disclination cores. This suggests that the so-called ordered texture[9] may contain defects with dimensions smaller than the resolution of optical microscopes.

These two principal orientations of the director, along the vorticity axis and along the flow direction, can be compared with the theoretical results of Larson and Öttinger.[5] They show the existence of the same two director attractors at low shear rates, the vorticity axis and the shearing plane.

Conclusions

New methods have been used to characterize the defects of the worm texture. As far as our results suggest, it is composed of twist disclination lines. Half-integer lines form loops lying inside the shearing plane, sometimes connected to integer lines oriented in the flow direction. This picture is coherent with what is known of the rheology of thermotropic polymers, for example the existence of two stable director positions, one in the flow direction and one in the vorticity axis, and the increase of loop density and orientation in the flow direction.

The results of this work raise many questions. The mechanism(s) at the origin of the creation of these loops remains to be found. The experimental method used here is not very well adapted to this study since it is a destructive one. A complete characterization of the director arrangement between neighboring loops is also lacking as well as the influence of these defects on the rheology. In particular, the gradual transition from the wormlike region to the ordered region is of considerable interest but still unknown.

References and Notes

(1) Graziano, D. J.; Mackley, M. R. *Mol. Cryst. Liq. Cryst.* **1984**, *106*, 73.
(2) Takebe, T.; Hashimoto, T.; Ernst, B.; Navard, P.; Stein, R. *J. Chem. Phys.* **1990**, *92*, 1386.
(3) Doi, M. *J. Polym. Sci., Polym. Phys. Ed.* **1981**, *19*, 229.
(4) Marrucci, G.; Maffetone, P. L. *Macromolecules* **1989**, *22*, 4076.
(5) Larson, R. G.; Öttinger, H. C. *Macromolecules* **1991**, *24*, 6270.
(6) Marrucci, G.; Greco, F. *J. Non-Newtonian Fluid Mech.* **1992**, *44*, 1.
(7) Friedel, J. *Dislocations*; Pergamon Press: New York, 1964.
(8) De'Nève, T.; Kléman, M.; Navard, P. *J. Phys. II Fr.* **1992**, *2*, 187.
(9) De'Nève, T.; Navard, P.; Kléman, M. *J. Rheol.* **1993**, *37*, 515.
(10) De'Nève, T.; Kléman, M.; Navard, P. *C. R. Acad. Sci. Paris* **1993**, *316*, (*II*), 1037.
(11) De'Nève, T.; Kléman, M.; Navard, P. Observation of Textures of Nematic Polymers and Estimation of Elastic Constants. *Liq. Crys.*, to appear.
(12) De'Nève, T. Relations entre Structure, Défauts et Rhéologie d'un Cristal Liquide Polymère Nématique Polymère, Ph.D. Dissertation, Ecole Nationale Supérieure des Mines de Paris, 1993.
(13) Hanna, S.; Lemmon, T. J.; Spontak, R. J.; Windle, A. H. *Polymer* **1992**, *33*, 3.
(14) Hudson, S.; Lovinger, A. J. *Polymer* **1993**, *34*, 1123.
(15) Bedford, S. E.; Windle, A. H. *Polymer* **1990**, *31*, 616.
(16) Hudson, S.; Lovinger, A. J.; Ventakaraman, S.; Manzione, L. T.; Liu, C. *Polymer Eng. Sci.* **1994**, *34*, 1328.
(17) Kléman, M.; Friedel, J. *J. Phys.* **1969**, *30* (C4), 43.
(18) Mazelet, G.; Kléman, M. *Polymer* **1986**, *27*, 714.
(19) Hudson, S. D.; Larson, R. G. *Phys. Rev. Lett.* **1993**, *70*, 2916.
(20) Geurst, J. A.; Spruijt, A. M. J.; Gerritsma, C. J. *J. Phys.* **1975**, *36*, 653.
(21) Cladis, P. E.; Kléman, M. *J. Phys.* **1972**, *33*, 591. Meyer, R. *Philos. Mag.* **1973**, *27*, 405.
(22) Marrucci, G.; Guido, S., in preparation.
(23) Larson, R. G.; Mead, D. W. *Liq. Cryst.* **1993**, *15*, 151.
(24) Moldenaers, P. Ph.D. Dissertation, Katholieke Universiteit, Leuven, 1987.
(25) Ernst, B.; Navard, P.; Hashimoto, T.; Takebe, T. *Macromolecules* **1990**, *23*, 1370.
(26) Riti, J. B.; Navard, P. *Synth. Polym. J.*, to appear.
(27) Patlazhan, S.; Riti, J. B.; Navard, P., in preparation.
(28) Keates, P.; Mitchell, G. R.; Peuvrel-Disdier, E.; Navard, P. *Polymer* **1993**, *34*, 1316.
(29) Keates, P.; Mitchell, G. R.; Peuvrel-Disdier, E.; Navard, P. *J. Non-Newtonian Fluid Mech.* **1994**, *52*, 197.
(30) Windle, A. Proceedings of the 16th Biennial Meeting on Physical Aspects of Polymer Science, Reading, UK, Sept 15–17, 1993.

MA941092D